Au Nanoparticle-Based Surface Energy Transfer Probe for Conformational Changes of BSA Protein

ARTICLE *in* THE JOURNAL OF PHYSICAL CHEMISTRY C · OCTOBER 2008

Impact Factor: 4.77 · DOI: 10.1021/jp806866r

3 AUTHORS, INCLUDING:

Krishna Kanta Haldar
Central University of Punjab
16 PUBLICATIONS **398** CITATIONS
SEE PROFILE

Amitava Patra
Indian Association for the Cultivation of Sci…
172 PUBLICATIONS **4,129** CITATIONS
SEE PROFILE

Au Nanoparticle-Based Surface Energy Transfer Probe for Conformational Changes of BSA Protein

Tapasi Sen, Krishna Kanta Haldar, and Amitava Patra*

Department of Materials Science and Center for Advanced Materials, Indian Association for the Cultivation of Science, Kolkata 700 032, India

Received: August 1, 2008

In the present study, Au nanoparticle based surface energy transfer (SET) has been used to measure conformational changes in proteins. A significant photoluminescence (PL) quenching (91−97%) of tryptophan intensities of bovine serum albumin (BSA) protein is observed in the presence of Au nanoparticles, and the measured distances (r) between the donor (tryptophan) and the acceptor (Au nanoparticle) are 27.0, 22.9, and 25.7 Å for E, N, and B forms of BSA protein, respectively. Results indicate that Au nanoparticle quenches BSA fluorescence mainly through a static quenching mechanism. Analysis suggests that binding constant and bound/unbound ratio varies with changing the conformation of protein. The PL quenching of dye varies from 47.2 to 86.6% with changing the conformation of protein without changing the radiative rate of dye. The measured distances (d) between the donor (dye) and the acceptor (Au nanoparticle) are 116.5, 76.1, and 86.4 Å for E, N, and B forms of BSA protein, respectively, using the efficiency of surface energy transfer (SET) which follows $1/d^4$ distance dependence. The estimated radii of different conformations of the protein nicely match with the reported values of hydrodynamic radii of different conformations of BSA protein. Therefore, such bioconjugated Au nanoparticle based surface energy transfer should have great potentials for optical-based molecular ruler.

Introduction

A variety of spectroscopic methods such as circular dichroism (CD), Fourier transform infrared (FTIR) spectroscopy, and fluorescence spectroscopy have been widely used to characterize the protein conformational changes.[1−5] Fluorescence resonance energy transfer (FRET) has been extensively used to measure conformational changes in proteins because the efficiency of FRET is very sensitive to measure the distance between a donor and an acceptor.[4] Recently, Weiss demonstrated the study of conformational dynamics of biomolecules by novel single molecule fluorescence spectroscopy.[5] Bovine serum albumin (BSA) is a commonly studied protein and is extensively used in biochemical studies. [6] It is a single polypeptide chain composed of 583 amino-acid residues, and its secondary structure is highly α-helical. The tertiary structure of BSA is comprised of three homologous domains, two tryptophans at position 134 and 213 with cysteine residues forming disulfide bonds. The conformation of BSA can undergo structural changes very easily with changing the pH values.[6,7] The normal or native forms of albumin is "N", which is predominant at neutral pH; "B" is for the basic form occurring above pH 8.0; "F" is for fast migrating form produced at pH below 4.0. "E" is for expanded form at pH less than 3.5, and "A" is for aged form produced at pH greater than 8.0. All of these conformational states have their own molecule dimensions and shape. Recently, the research in bioconjugated nanoparticles is one of the most emerging areas of nanotechnology because of their promising applications such as luminescence tagging, imaging, medical diagnostics, multiplexing, and most recently as biosensors. Several studies[8−11] on the BSA conjugated nanoparticles have been reported. Ren et al.[8] demonstrated the synthesis of silver sulfide nanorods conjugated with BSA. Such conjugation was reported to increase the luminescence intensities of the CdTe nanoparticles, and the enhancement of luminescence intensities was attributed to the resonance energy transfer from the tryptophan moieties of protein to CdTe nanoparticles.[9] Shang et al.[11] reported pH dependent conformational changes of Au nanoparticle conjugated BSA protein by spectroscopic study.

A significant attention has been paid on the QD based Förster resonance energy transfer (FRET) due to their narrow emission and broad excitation spectra. The ability of tuning of emission properties with changing size may allow for efficient energy transfer with a number of organic dyes.[12] Medintz et al.[12] reported the potential of luminescent semiconductor quantum dots for development of hybrid inorganic-bio receptor sensing materials. They demonstrated the use of luminescent CdSe-ZnS QDs as energy donors in FRET based assays with organic dyes as energy acceptors in QDs-dye labeled protein conjugates. In most cases, the energy transfer in QD conjugates is discussed as a FRET process. FRET occurs when the electronic excitation energy of a donor fluorophore is transferred to a nearby acceptor molecule, and the transfer efficiency increases with increasing the spectral overlap between the donor emission and the acceptor absorption. The efficiency of FRET depends on the distance of separation between donor and acceptor molecules. According to the Förster theory, the rate of energy transfer is given by[13,14]

$$k_T(r) = \frac{1}{\tau_D}\left(\frac{R_0}{r}\right)^6 \quad (1)$$

where τ_D is the lifetime of the donor in the absence of the acceptor, r is the distance between the donor and the acceptor, and R_0 is known as the Förster distance, the distance at which the transfer rate $k_T(r)$ is equal to the decay rate of the donor in absence of the acceptor.

* Author to whom correspondence should be addressed. E-mail: msap@iacs.res.in. Phone: (91)-33-2473-4971. Fax: (91)-33-2473-2805.

10.1021/jp806866r CCC: $40.75
Published on Web 10/23/2008

Recently, the energy transfer between Au nanoparticle and dye provides a new paradigm for design of optical based molecular ruler for long distance measurement.[15−23] Gold nanoparticles are used to be acceptors in biophysical experiments in vitro as well as in vivo. Several theoretical studies have been published on energy transfer from a dye to metal surface, and they have demonstrated the mechanism of dye quenching at a metal surface and the separation of donor and acceptor is d^{-4} dependence.[24−27] According to the model, the exact form of dipole−surface energy transfer (SET) rate is given by

$$k_{SET} = \frac{1}{\tau_D}\left(\frac{d_0}{d}\right)^4 \tag{2}$$

Thus, SET process is an useful spectroscopic ruler for long distance measurement which will help to understand the large scale conformational dynamics of complex biomolecules in macroscopic detail. Dulkeith et al.[18] showed the change of radiative and nonradiative decay rates of the chemically attached dye molecules with different sized gold nanoparticles. Strouse et al.[15−17] reported the surface energy transfer (SET) from dye to DNA attached Au nanoparticle, and the energy transfer process follows $1/d^4$ distance dependence. In our previous study, we also reported the efficient surface energy transfer process from dye to different shaped Au nanoparticle.[18−20] Ray et al.[23] demonstrated the ultrasensitive detection of mercury in soil, water, and fish using the surface energy transfer process. To the best of our knowledge, there has been no such study on conformational changes of protein conjugated nanoparticles using surface energy transfer method where Au nanoparticles act as acceptor and dye molecules act as donor. Such Au nanoparticles may have great potentials for optical-based molecular ruler. This study represents an initial attempt to understand the change of conformational of BSA protein conjugated Au nanoparticles with varying pH values. We are addressing the following issues: can these BSA conjugated Au nanoparticles be efficient quenchers? What kind of quenching mechanism (static or dynamic) is involved? How do the binding constant and bound/unbound ratio's vary with changing the conformation?

Experimental Procedures

Chloroauric acid ($HAuCl_4 \cdot 3H_2O$, S.d.Fine Chem), sodium borohydride ($NaBH_4$, Merck), Bovine serum albumin (BSA, Sigma) and Rhodamine 6G dye (Aldrich) were used without further purification.

Synthesis of BSA Conjugated Gold Nanoparticles. BSA-conjugated gold nanoparticles at different pH were prepared using modified reported methods.[10] For the preparation of BSA-conjugated Au nanoparticles at pH 7.0, 0.1 μmol BSA (0.0066 g) was dissolved in 9.5 mL PBS buffer solution of pH 7.0. Then, 0.5 mL of 10 mM $HAuCl_4$ solution was added into the BSA-buffer solution. After 5 min stirring, 100 μL of ice cold $NaBH_4$ aqueous solution (0.001 g/mL) was added to the BSA solution slowly under constant stirring. The solution color changes from light yellow to reddish brown. Other bioconjugated Au nanoparticles were prepared at pH 3.0 and 9.0 by adding HCl or NaOH solution to the as-prepared gold nanoparticle solution at pH 7.0. The colors of the Au nanoparticle solutions remain the same after adjusting the pH at 3.0 and 9.0. All of the colloidal solutions were stored at 4 °C prior to use. The concentration of the as-prepared Au nanoparticle solution was calculated to be 1.24×10^{-7} M under the assumption that all Au^{3+} ions converted to Au^o. No separation technique to extract the excess protein in the bioconjugates was used because this may disrupt the original conformation of the protein in the bioconjugates. A 0.5 mL sample of 1 μM R6G solution was added to 3.0 mL each of the colloidal bioconjugated Au solutions. All of the solutions were kept for 1 day for stabilization. After 1 day, dye containing BSA conjugated Au solutions were used for optical study.

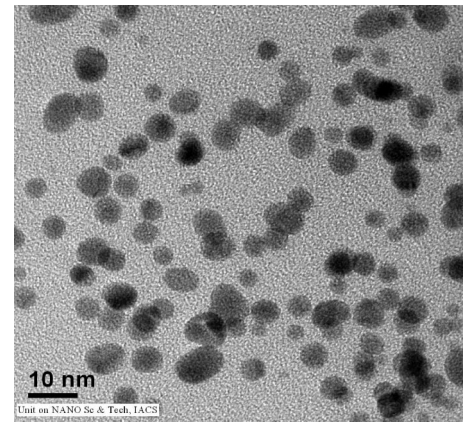

Figure 1. TEM image of Au nanoparticles at pH 7.0.

The transmission electron microscopy (TEM) images were taken using a JEOL-TEM-2010 transmission electron microscope with an operating voltage of 200 kV. Room-temperature optical absorption spectra were obtained with a UV−vis spectrophotometer (Shimadzu). CD spectra were taken on a JASCO J-815 CD spectrometer (J-815−150S) with a rectangular quartz cell having 1.0 mm path length. All CD spectra were taken in a wavelength range of 200−250 nm, and each spectrum was the accumulation of three scans. The emission spectra of all samples were recorded in a fluoro Max-P (Horiba Jobin Yvon) luminescence spectrophotometer. For the time correlated single photon counting (TCSPC) measurements, the samples were excited at 405 nm using a picoseconds diode laser (IBH Nanoled-07) in an IBH Fluorocube apparatus. The typical full width at half-maximum (fwhm) of the system response using a liquid scatter is about 90 ps. The repetition rate is 1 MHz. The fluorescence decays were collected on a Hamamatsu MCP photomultiplier (C487802). The fluorescence decays were analyzed using IBH DAS6 software. The following expression was used to analyze the experimental time-resolved fluorescence decays, $P(t)$:

$$P(t) = b + \sum_i^n \alpha_i \exp(-t/\tau_i) \tag{3}$$

Here, n is the number of discrete emissive species; b is a baseline correction ("dc" offset), and α_i and τ_i are the pre-exponential factors and excited-state fluorescence lifetimes associated with the ith component, respectively. For biexponential decays ($n = 2$), the average lifetime, $\langle\tau\rangle$, was calculated from

$$\langle\tau\rangle = \sum_{i=1}^{2} \alpha_i\tau_i^2 / \sum_{i=1}^{2} \alpha_i\tau_i \tag{4}$$

Results and Discussion

Transmission Electron Microscopy. Figure 1 shows the TEM images of BSA conjugated Au nanoparticles at pH 7.0. The image clearly shows the nearly spherical shape of the particles having an average diameter of 5.4 ± 0.6 nm. The EDS spectrum of the protein films (S1, Supporting Information)

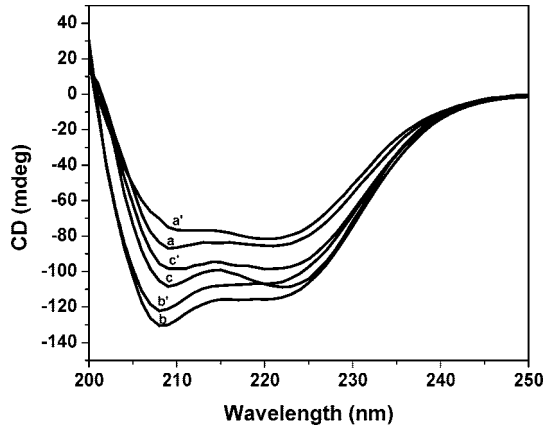

Figure 2. CD spectra of 1×10^{-5} M native BSA (curve a, b, c) and the corresponding Au-conjugated BSA (curve a′, b′, c′) at pH 3.0, 7.0, and 9.0, respectively. The concentration of Au nanoparticles was 1.24×10^{-7} M in each pH.

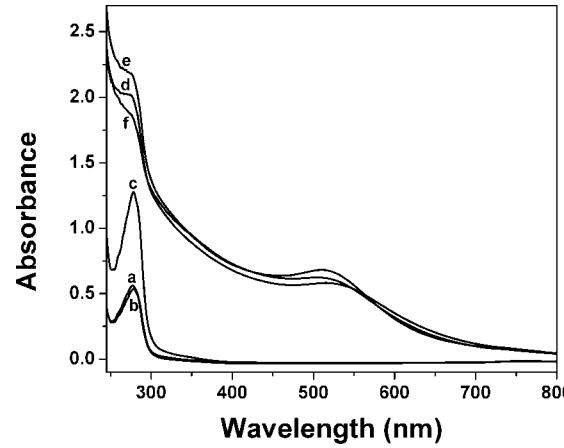

Figure 3. Absorption spectra of 1×10^{-5} M BSA in the absence (curves a−c) and in presence of Au nanoparticles (curves d−f) at pH 3.0, 7.0, and 9.0, respectively. The concentration of Au nanoparticles was 1.24×10^{-7} M in each pH.

confirms the presence of C, N, O, S, and Au. The Cu is from the TEM grid. The S:Au ratio indicates that gold nanoparticles bind with the protein, which is consistent with an earlier report.[10]

Dynamic Light Scattering (DLS) Study. DLS measurement was performed with the BSA solution of 1×10^{-5} M concentration, before and after conjugation with Au nanoparticles. DLS data give the hydrodynamic diameter of 12.4 and 18.8 nm for pure BSA and Au-conjugated BSA at pH 7.0 (shown in S2A,B, Supporting Information), respectively. Thus, it reveals that the hydrodynamic diameter of Au nanoparticles may be 6.4 nm, which matches with the TEM data (5.4 nm) with some error of +18%.

Circular Dichroism (CD) Study. CD spectroscopy is one of the commonly used methods to study the protein conformations in solution or adsorbed onto colloidal surfaces.[1] Figure 2 shows the far-UV CD spectra of native BSA and the corresponding Au-BSA at pH 7.0, 3.0, and 9.0. The CD spectra of native BSA at pH 7.0 exhibits two negative minima in the ultraviolet region at 208 and 222 nm, which are characteristic of an α-helical structure of protein.[1] The highest helicity occurred at pH 7.0 which corresponded to the normal (N) form of the albumin, with a larger decrease at pH 3.0 (E form) and a smaller decrease at pH 9.0 (B form). This change in the helicity of BSA at different pH values mostly originated from the different conformational states. In the N form, BSA possess the more compact form, while in N−E transition or N−B transition, the BSA molecule underwent an expansion.[1] Since the α helix is one of the elements of secondary structure of protein, the decrease in α helicity from N to B form and N to E form means a loss of the secondary structure. To understand the conformational behavior of BSA in the BSA-Au conjugates, CD measurement was performed. All of the CD data were analyzed by K2D software, and the percentage of α helices were obtained to be 52%, 62%, and 60% respectively for pure BSA at pH 3.0, 7.0, and 9.0, respectively. The results were in good agreement with that reported previously.[11] The spectra show that the helicity of the Au conjugated BSA decreases slightly at each pH. The helicity of BSA in the bioconjugates are calculated to be 50%, 59%, and 57% at pH 3.0, 7.0, and 9.0, respectively. The small decrease in helicity (∼3%) indicates that the secondary structure and the tertiary structure of BSA remain almost intact after bioconjugation, which is essential for the preparation of protein-based assemblies of NPs.[9]

Steady-State Study. Figure 3 shows the absorption spectra of native BSA in PBS and BSA-conjugated Au nanoparticles at pH 3.0, 7.0, and 9.0. As shown in curves a, b, and c, pure BSA exhibits an absorption maximum at 278 nm, which originates from the aromatic residues tryptophan and tyrosine and the disulfide bonds in the protein. The position of the absorption peak remains almost unchanged after the conjugation of BSA with Au nanoparticles at either pH, although the shape of the band changed slightly. From the absorption spectra, any valuable information relevant to the conformational behavior of the BSA protein in the bioconjugates is difficult to extract because of the substantial contribution of Au nanoparticles in this region.[11] In the absorption spectra, the bioconjugated Au nanoparticles prepared at pH 7.0 showed the surface plasmon band centered at 505 nm. It is well-known that BSA is rich in amino moieties and also contains several disulfide bonds with one free thiol in the cysteine residues.[28] These functionalities are probably responsible for the conjugation of Au nanoparticles via thiolate linkage and/or weak covalent bonds with alkylamines. More specific local information can be obtained for the protein with intrinsic fluorescence by selectively exciting the tryptophan (Trp) residues. BSA possesses two Trp residues, one residing on the bottom of hydrophobic pocket in domain II (Trp-213) and the other is on the surface of the molecule in domain I (Trp-134).[6] Thus, the information of the protein conformational behavior can be obtained from the emission spectra of Trp in the bioconjugates. Figure 4 shows the PL spectra of native BSA and BSA-conjugated Au nanoparticles at different pH values upon excitation at 295 nm. Excitation wavelength of 295 nm was taken to avoid the contribution from the tyrosine residues. The emission peaks are at 341, 352, and 350 nm for pH 3.0 (E), 7.0 (N), and 9.0 (B), respectively, indicating different conformational states of BSA. From the emission spectra of BSA-conjugated Au nanoparticles, it is clear that the tryptophan fluorescence was drastically quenched in presence of Au nanopaticles at either pH, which implies that efficient energy transfer takes place between BSA and Au nanoparticles. It reveals that Au nanoparticles reside near tryptophan of the BSA protein molecule, which is consistent with an earlier report.[11] It is well-known that this protein spontaneously binds a variety of hydrophobic fluorophores. In the present study, we did not observe any change in PL intensity of dye molecule (Rh6G) in presence of BSA protein. As Rhodamine 6G is a hydrophilic dye, it is located in the polar region of the protein, that is, on the surface of the protein exposed to the polar solvent.

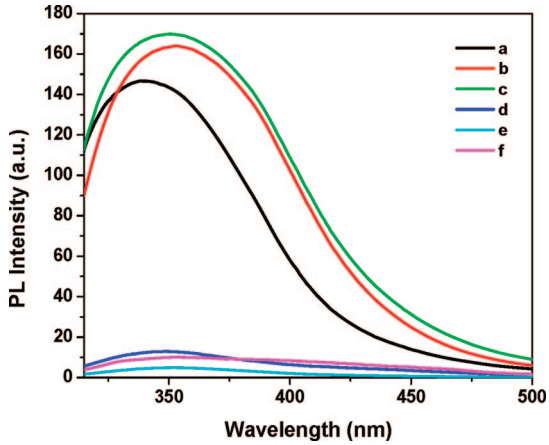

Figure 4. Fluorescence spectra of 1×10^{-5} M BSA in the absence (curves a−c) and in presence of Au nanoparticles (curves d−f) at pH 3.0, 7.0, and 9.0, respectively, upon excitation at 295 nm at pH 7.0 in 0.01 M PBS. The concentration of Au nanoparticles was 1.24×10^{-7} M in each pH.

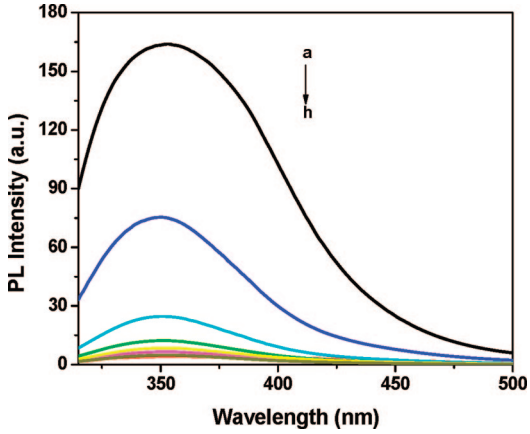

Figure 5. Photoluminescence spectra of 1×10^{-5} M BSA in the absence (curve a) and in presence of Au nanoparticles with increasing concentrations in the range from 1.03×10^{-8} M to 1.24×10^{-7} M (curves b−h) upon excitation at 295 nm at pH 7.0 in 0.01 M PBS.

We studied the fluorescence quenching of trytophan with changing the quencher (Au nanoparticle) concentration. A gradual quenching of the fluorescence intensity of tryptophan with increasing concentration of Au nanoparticles at pH 7 is seen in Figure 5. On the basis of the relationship between quenching of excited states and quencher concentration, the Stern−Volmer equation is given by[14]

$$\frac{F_0}{F} = 1 + K_q\tau_0[Q] = 1 + K_{SV}[Q] \qquad (5)$$

Here, F_0 and F are the relative fluorescence intensity in absence and presence of quencher, respectively. K_q is the bimolecular quenching rate constant; τ_0 is the average lifetime of the fluorophore in the absence of quencher, and [Q] is the concentration of the quencher. K_{SV} is the Stern−Volmer quenching constant which measures the efficiency of quenching. Figure 6 shows the Stern−Volmer plots of F_0/F versus [Au nanoparticles] at pH 7.0 (a), at pH 9.0 (b), and at pH 3.0 (c). By the linear fitting of the data, the calculated K_{SV} values are 30.45×10^7 M^{-1}, 12.86×10^7 M^{-1}, and 8.31×10^7 M^{-1}, for pH 7.0, 9.0, and 3.0, respectively. For BSA, τ_0 is known to be $\sim 5 \times 10^{-9}$ s. Thus, from eq 5, the values of K_q are calculated to be 6.09×10^{16} M^{-1} s^{-1}, 2.57×10^{16} M^{-1} s^{-1}, and 1.66×10^{16} M^{-1} s^{-1} for the bioconjugates at pH 7.0, 9.0, and 3.0,

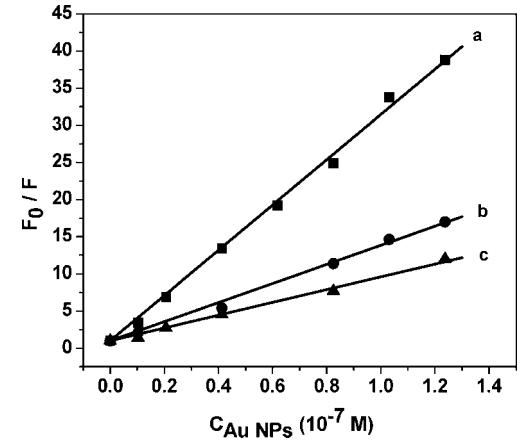

Figure 6. Stern−Volmer plot of Au conjugated BSA at pH 7.0 (a), at pH 9.0 (b), and at pH 3.0 (c). The concentration of BSA was 1×10^{-5} M and the concentration of Au nanoparticles varies from 1.03×10^{-8} M to 1.24×10^{-7} M in all cases.

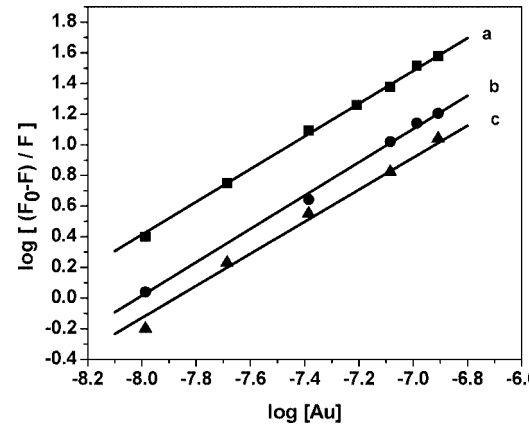

Figure 7. Plot of log $[(F_0 - F)/F]$ vs log [Au] for Au conjugated BSA at pH 7.0 (a), at pH 9.0 (b), and at pH 3.0 (c).

respectively, since the maximum value of K_q for a diffusion-controlled quenching process[14] with biopolymer is about 2.0×10^{10} M^{-1} s^{-1}. The higher value quenching rate constants imply that it is a static quenching process. Static quenching arises only from the formation of complex between BSA and Au nanoparticles. For the static quenching process, under the assumption that BSA has the same and independent binding sites, the following equation was found for the determination of binding constant or association constant (K_A) and binding sits (n):[29]

$$\log[(F_0 - F)/F] = \log K_A + n\log[Au] \qquad (6)$$

Figure 7 shows the plot of log $[(F_0 - F)/F]$ versus log [Au] for the Au conjugated BSA at pH 7.0 (a), at pH 9.0 (b), and at pH 3.0 (c). From the slope of the linear fitting plots, binding site numbers, n, were found to be 1.07, 1.09, and 1.04 at pH 7.0, 9.0, and 3.0, respectively, and from the intercept (log K_A), the binding constants, K_A, were calculated to be 9.12×10^8 M^{-1}, 5.13×10^8 M^{-1}, and 1.66×10^8 M^{-1}, at pH 7.0, 9.0, and 3.0, respectively. Thus, it was found that the binding constant at pH 7.0 is larger than those at pH 9.0 and 3.0 while the binding sites are almost similar at different pH values. The calculated bound-to-unbound ratios are 37.8, 16.0, and 11.0 for pH 7.0, 9.0, and 3.0, respectively, using fixed particle concentration of Au (1.24×10^{-7} M). It reveals that the binding constant and the bound/unbound ratio vary with changing the conformation of protein, and Au nanoparticles are suitable for binding to the BSA molecule in the neutral condition.

The observed quenching of PL intensities are 91.7%, 97.1%, and 94.1% for E, N, and B forms of BSA protein, respectively (Figure 4). We estimated the distance between donor and acceptor using FRET method. Förster distance (R_0) is calculated from the relation

$$R_0 = 0.211[\kappa^2 n^{-4} \varphi_{dye} J(\lambda)]^{1/6} \quad (7)$$

where κ^2 is the orientation factor, $\phi_{tryptophan}$ is the quantum efficiency of tryptophan (0.118), $J(\lambda)$ is the overlap integral between the absorption peak of acceptor (Au nanoparticle) and the emission peak of donor (tryptophan), and n is the refractive index of the medium. The calculated Förster distances (R_0) are 40.3, 41.2, and 40.8 Å, and the corresponding estimated distance (r) between the donor and the acceptor are 27.0, 22.9, and 25.7 Å for E, N, and B forms of BSA protein, respectively, using the FRET method (eq 1). Sahu et al.[30] reported that the ANS binding site in BSA is at a distance of 27 Å from tryptophan. Tian and co-worker[31] reported that the distance between donor−acceptor (r) for BSA-BAR system was 28.4 Å at pH 7.0. Lakowicz et al.[32] reported a dramatic increases in the Förster distance from 28.6 to 63 Å during the energy transfer from BSA to silver particles. As it is energy transfer from tryptophan to Au nanoparticles, therefore, we also used the surface energy transfer (SET) method for calculating the distance between donor and acceptor, and d_0 value is calculated using Persson model[25]

$$d_0 = \left(\frac{0.225 c^3 \Phi_d}{\omega_d^2 \omega_F k_F}\right)^{1/4} \quad (8)$$

where d_0 is the distance at which a dye will display equal probabilities for energy transfer and spontaneous emission. ϕ_d is the quantum efficiency of tryptophan (0.118); the frequency of the donor electronic transition is ω, and the Fermi frequency is ω_F, and the Fermi wave vector is k_F of the metal.[15] The d_0 value was calculated using $\phi_{dye} = 0.118$, $\omega = 6.8 \times 10^{15}$ s^{-1}, $\omega_F = 8.4 \times 10^{15}$ s^{-1}, $k_F = 1.2 \times 10^8$ cm^{-1}, and $c = 3 \times 10^{10}$ cm s^{-1}. The calculated d_0 value is 35.2 Å for BSA-conjugated Au nanoparticles prepared at pH 3.0, 7.0, and 9.0, respectively. The quantum efficiency of energy transfer in surface energy transfer process can be written as

$$\varphi_{ET} = \frac{1}{1 + \left(\frac{d}{d_0}\right)^4} \quad (9)$$

The calculated distances (d) between the donor and the acceptor are 19.1, 14.6, and 17.7 Å for E, N, and B forms of BSA protein, respectively, using the efficiency of SET which depends on the inverse fourth power of the distance of separations between donor and acceptor (eq 9). The results show that Au nanoparticles are strong quenchers and they are situated at close proximity to the tryptophan residue. Results indicate that Au nanoparticles quench BSA fluorescence mainly through a static quenching mechanism.

A drastic quenching in PL intensity of R6G emission in presence of BSA conjugated Au nanoparticles is observed in Figure 8. The observed quenching of PL intensities of dye are 47.2%, 86.6%, and 80.5% for E, N, and B forms of BSA protein, respectively, indicating the quenching process depends on the conformation of protein which varies with pH values. To understand the origin of the quenching process, we calculate the radiative rate (k_r) by using the following relation[15]

$$k_r = 3.13 \times 10^{-9} \nu_0^2 \int \varepsilon d\bar{\upsilon} \cong \nu_0^2 f \quad (10)$$

where ν_0 is the energy in wavenumbers corresponding to the maximum absorption of the dye, ε is the extinction coefficient, and f is the oscillator strength. The absorption spectra of R6G in absence and in presence of Au nanoparticles bioconjugated with BSA at different pH is shown in Figure S3. The calculated radiative rate of the dye at different pH values are 5.4 × 10^7 s^{-1}, 4.32 × 10^7 s^{-1}, and 4.5 × 10^7 s^{-1} in absence of Au nanoparticles at pH 3.0, pH 7, and pH 9, respectively. The calculated radiative rates are 5.35 × 10^7 s^{-1}, 4.23 × 10^7 s^{-1}, and 4.44 × 10^7 s^{-1} for E, N, and B forms of BSA protein, respectively. It indicates a very small change in radiative rate. The change in the oscillator strength is 1−3% which is much less compared with quenching of PL intensity (47.2%, 86.6%, and 80.5%). Therefore, the PL quenching of the dye is definitely due to the energy transfer process.

Time-Resolved Fluorescence Study. The time-resolved fluorescence spectra of aqueous solution of pure R6G dye and in presence of BSA-conjugated Au nanoparticle at different pH values are shown in Figure 9. The photoluminescence decay time of the dye solution (1 μM) at different pH without Au nanoparticle is single exponential, and the value is 3.92 ns, which is for unbound dye molecules. However, the fluorescence decay of dye in presence of BSA conjugated Au nanoparticles to a biexponential function was used instead of a stretched exponential because it provided better agreement (Table 1). If

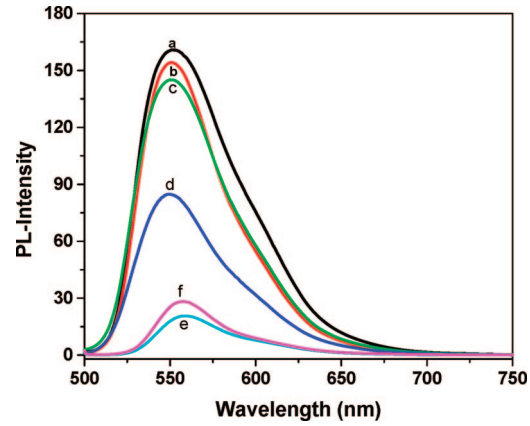

Figure 8. Photoluminescence (PL) spectra of 1 μM Rhodamine 6G (R6G) dye solution (a) at pH 3, (b) at pH 7.0, (c) at pH 9.0, and in presence of Au nanoparticles (d) at pH 3.0, (e) at pH 7.0, and (f) at pH 9.0.

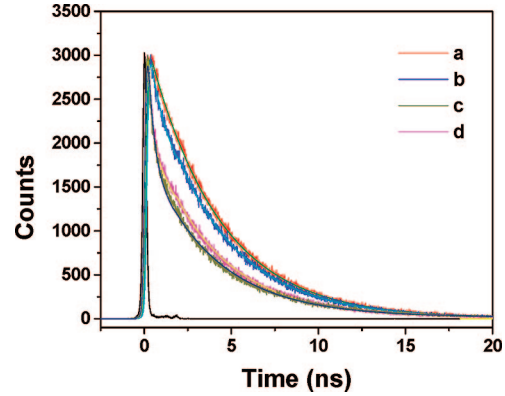

Figure 9. Decay curves of (a) 1 μM Rhodamine 6G (R6G) dye solution in pure BSA at pH 7.0, (b) Au-BSA at pH 3.0 and 1 μM R6G, (c) Au-BSA at pH 7.0 and 1 μM R6G, and (d) Au-BSA at pH 7.0 and 1 μM R6G.

TABLE 1: Time Resolved Fluorescence Quenching Studies for Different Rh6G-Au Nanoparticles Pairs

system	b_1	τ_1 (ps)	b_2	τ_2 (ns)	$\langle\tau\rangle = (b_1\tau_1 + b_2\tau_2)$ (ns)	E (%)
Rh6G in blank BSA at pH 3, pH 7 and pH 9			1.0	3.92	3.92	
Rh6G in BSA-conjugated Au nanoparticles at pH 3	0.22	500	0.78	3.91	3.16	19.4
Rh6G in BSA-conjugated Au nanoparticles at pH 7	0.56	178	0.44	3.65	1.70	56.6
Rh6G in BSA-conjugated Au nanoparticles at pH 9	0.49	419	0.51	3.87	2.18	44.2

TABLE 2: Energy Transfer Parameters for Different Rh6G-Au Nanoparticles Pairs

system	λ_{em} (nm)	J(λ) (M^{-1} cm^{-1} nm^4)	Φ^0_D	E(%) (PL)	R_0 (Å)	r (Å)	d_0 (Å)	d (Å)
Rh6G in blank BSA solution at pH 3	551		0.952					
Rh6G in BSA-Au nanoparticles at pH 3	549	1.08×10^{17}	0.952	47.2	107.8	136.7	81.6	116.5
Rh6G in blank BSA solution at pH 7.0	550		0.940					
Rh6G in BSA-Au nanoparticles at pH 7.0	560	8.43×10^{16}	0.940	86.6	103.3	98.8	81.3	76.1
Rh6G in blank BSA solution at pH 9.0	550		0.950					
Rh6G in BSA-Au nanoparticles at pH 9.0	558	1.01×10^{17}	0.950	80.5	106.7	110.9	81.5	86.4

the intensity decays are multiexponential, then it is important to use an average decay time which is proportional to the steady-state intensity.[14] The average values are given by the sum of the $\sum b_i\tau_i$ products. The fast and slow components are 500 ps (22%) and 3.91 ns (78%) for the dye solution (1 μM) in presence of BSA-conjugated Au prepared at pH 3.0 (Table 1). We attribute the slow component (3.91 ns) to unbound dye molecules and attribute the fast component (500 ps) to bound dye molecules.[18] The fast and slow components are 178 ps (56%) and 3.65 ns (44%) for the dye solution in presence of BSA-conjugated Au nanoparticles at pH 7.0 (Table 1). Here, the slow component decay time 3.65 ns is attributed to unbound dye, and the fast component 178 ps is attributed to bound dye molecules. The fast and slow components are 419 ps (49%) and 3.87 ns (51%) for the dye solution in presence of BSA-conjugated Au nanoparticles prepared at pH 9.0 (Table 1). Similarly, the slow component decay time 3.87 ns is attributed to unbound dye, and the fast component 419 ps is due to bound dye molecules. The average decay times are 3.16, 1.70, and 2.18 ns for BSA-conjugated Au nanoparticles prepared at pH 3.0, 7.0, and 9.0, respectively (eq 2). The shortening of the decay time of dye in presence of Au again confirms the energy transfer from dye to Au nanoparticles. Dulkeith et al.[18] observed similar results in dye containing Au nanoparticles where the fluorescence lifetime decreases in presence of Au nanoparticles. Lifetime measurement is more sensitive than PL quenching efficiency because error comes from the fluctuations in lamp intensity. Therefore, the energy transfer efficiency from dye to Au nanoparticles is calculated by using the relation $\phi_{ET} = 1 - \tau_{DA}/\tau_D$, where τ_{DA} is the decay time of dye in presence Au nanoparticles and τ_D corresponds to the decay time of dye in absence of Au nanoparticles. The calculated energy transfer efficiencies from dye to Au nanoparticles are 19.4, 56.6, and 44.2% for BSA-conjugated Au nanoparticles prepared at pH 3.0, 7.0, and 9.0, respectively (Table 1), indicating the energy transfer is fastest in BSA-conjugated Au nanoparticles prepared at pH 7.0. The efficient energy transfer between Au nanoparticles and dye provides a basis for novel assay designs and multiplexing potential.

Figure 10 shows the efficiency ($E = 1 - \tau_{DA}/\tau_D$) of the quenching of dye as a function of the ratio between the molar concentrations of donors and and those of acceptors ($x = C_D/C_A$) for bioconjugated Au nanoparticle prepared at pH 7.0. It is clearly seen from the Figure 10 that the efficiency of quenching process increases monotonically with decreasing in x. It is noteworthy that the very effective quenching of dye characterized by $E = 0.57$ was observed for assemblies with x equal to 1. Analysis of the results reveals that single acceptor Au nanoparticles interact with single donor dye molecules for all three conformations.

We estimated the distance between donor (dye) and acceptor (Au nanoparticle), by using FRET and SET methods. We calculated the overlap integral [$J(\lambda)$] from the overlap of emission spectra of donor (dye) and absorption spectra of the acceptor, and the values are listed in Table 2. The calculated Förster distances (R_0) are 107.8, 103.3, and 106.7 Å, and the corresponding calculated distance (r) between the donor and the acceptor is 136.7, 98.8, and 110.9 Å for E, N, and B forms of BSA protein, respectively (Table 2), using the efficiency of FRET which depends on the inverse sixth power of the distance of separations between one donor and one acceptor. It is again already reported that the FRET based method is restricted on the upper limit of only 80 Å, because the energy transfer becomes too weak to be useful.[14] Again, we used the surface energy transfer method for calculating the distance between donor and acceptor using eq 9. The d_0 value was calculated using $\phi_{dye} = 0.952$, 0.94, and 0.95 at pH 3, 7, and 9, respectively; $\omega = 3.6 \times 10^{15}$ s^{-1}, $\omega_F = 8.4 \times 10^{15}$ s^{-1}, $k_F = 1.2 \times 10^8$ cm^{-1}, and $c = 3 \times 10^{10}$ cm s^{-1}. The calculated d_0 values are 81.6, 81.3, and 81.5 Å for E, N, and B forms of BSA protein, respectively (Table 2). The calculated distance (d) between the donor and the acceptor is 116.5, 76.1, and 86.4 Å for E, N, and B forms of BSA protein, respectively (Table

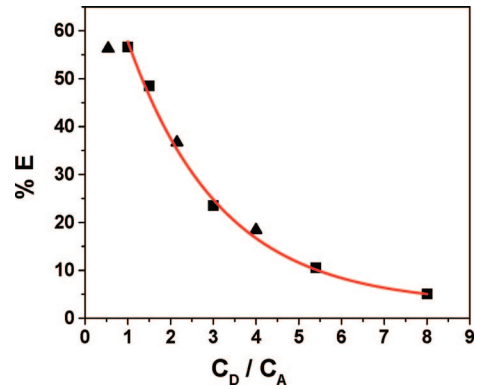

Figure 10. Dependence of the efficiency of quenching of R6G dye by BSA conjugated Au nanoparticles prepared at pH 7.0 from time-resolved data, $E = 1 - \tau/\tau_0$ as a function of the R6G dye to Au nanoparicle ratio (x). Squares are E values obtained in experiment where the concentration of donor (R6G) was maintained constant (1 μM), and the concn of acceptor (core−shell) was varied. Triangles correspond to the experiment where the concn of acceptor was maintained constant (1.3×10^{-7} M) and the concn of donor was varied. The solid line is fitting of data in a first order exponential decay.

2), using the efficiency of SET which depends on the inverse fourth power of the distance of separations between donor and acceptor (eq 9). As the FRET based method is restricted on the upper limit of only 80 Å, therefore, we may suggest that the energy transfer from dye to Au nanoparticles is the surface energy transfer (SET) process in the present study, and it follows $1/d^4$ distance dependence. The observed distance of closest approach was found to be in agreement with the conformational changes of BSA with pH. Here, we try to correlate the distance between donor and acceptor (d) with the hydrodynamic radius of protein. It is reported that the hydrodynamic radius at low pH increases above two-fold compared with neutral conditions, and in the basic solution, albumin is clearly expanded too. Recently, Huang et al.[33] measured the hydrodynamic diameter of CdTe(QD)-HRP conjugates and CdTe (QD) by fluorescence correlation spectroscopy, and the values are 8 and 4 nm, respectively. However, the reported hydrodynamic diameter of HRP is 3.5 nm, indicating the hydrodynamic diameter of HRP increases from 3.5 to 8.0 nm in presence of CdTe nanoparticles. Recently, Böhme and Scheler[34] determined the hydrodynamic radii of BSA protein with changing pH values by electrophoresis NMR study, and they reported hydrodynamic radii are 9.3, 4.5, and 6.0 nm for pH 2.4, 6.8, and 10.5, respectively. These changes in the hydrodynamic radius again reflect the changes in the conformation of the protein under variation of the pH. In the present study, the average radius of Au particle is 2.7 nm (TEM study), thus, the estimated radii of the protein at different conformations without Au nanoparticles are 9.0, 4.9, and 6.0 nm for pH 3.0, 7.0, and 9.0, respectively, which nicely matches with the reported values of hydrodynamic radii of BSA protein with different conformations.[34] Therefore, the distance between dye and bioconjugated Au nanoparticles has a strong correlation with the hydrodynamic size of the BSA protein. Therefore, the conformational changes in proteins can be studied by using surface energy transfer as a spectroscopic ruler.

Conclusion

To the best of our knowledge, this is the first report to study the conformational changes of BSA protein using Au nanoparticle based surface energy transfer (SET). The calculated energy transfer efficiencies from dye to nanoparticles are 19.4, 56.6, and 44.2% for BSA-conjugated Au nanoparticles prepared at pH 3.0, 7.0, and 9.0, respectively. Analysis suggests that the PL quenching of dye is mainly due to nonradiative decay channel without any significant modification of the radiative rate which confirms the resonant energy transfer process. The calculated distance (r) between the donor and the acceptor is 136.7, 98.8, and 110.9 Å for E, N, and B forms of BSA protein, respectively, using the efficiency of FRET which depends on the inverse sixth power of the distance of separations between single donor and single acceptor. However, the calculated distance (d) between the donor and the acceptor is 116.5, 76.1, and 86.4 Å for E, N, and B forms of BSA protein, respectively, using the efficiency of SET which depends on the inverse fourth power of the distance of separations between donor and acceptor. The estimated radii of the protein at different conformations without Au nanoparticles are 9.0, 4.9, and 6.0 nm for pH 3.0, 7.0, and 9.0, respectively, which nicely matches with the reported values of hydrodynamic radii of BSA protein with different conformations. Therefore, such bioconjugated Au nanoparticles could pave the way for designing new optical based materials for the application in chemical sensing or biological imaging.

Acknowledgment. A.P. thanks The Department of Science and Technology (NSTI) and "Ramanujan Fellowship" for generous funding. T.S. thanks CSIR for awarding fellowship. Subrata Das is acknowledged for his technical assistance.

Supporting Information Available: The EDS spectrum of the BSA conjugated Au nanoparticles at pH 7.0 (S1), the DLS spectra of pure BSA and the corresponding Au conjugated BSA at pH 7.0, the UV−visible spectra of 1 μM Rh6G dye solution in absence and presence of Au nanoparticles at different pH values, the PL spectra of 1 μM Rhodamine 6G (R6G) dye in 0.01 M PBS buffer solution at pH 3.0, 7.0, and 9.0 and in presence of 1×10^{-5} M BSA in 0.01 M PBS buffer solution at pH 3.0, 7.0, and pH 9.0. This information is available free of charge via the Internet at http:// pubs.acs.org.

References and Notes

(1) Greenfield, N. J. *Trends Anal. Chem.* **1999**, *18*, 236.
(2) Haris, P. I.; Chapman, D. *Trends Biol. Sci.* **1992**, *17*, 328.
(3) Royer, C. A. *Chem. Rev.* **2006**, *106*, 1769.
(4) Selvin, P. R. *Nat. Struct. Biol.* **2000**, *7*, 730.
(5) Weiss, S. *Nat. Struct. Biol.* **2000**, *7*, 724.
(6) Carter, D. C.; Ho, X. J. *Adv. Protein Chem.* **1994**, *45*, 153.
(7) Sogami, M.; Petersen, H. A.; Foster, J. F. *Biochemistry* **1969**, *8*, 49.
(8) Yang, L.; Xing, R.; Shen, Q.; Jiang, K.; Ye, F.; Wang, J.; Ren, Q. *J. Phys. Chem. B* **2006**, *110*, 10534.
(9) Mamedova, N. N.; Kotov, N. A.; Rogach, A. L.; Studer, J. *Nano Lett.* **2001**, *1*, 281.
(10) (a) Burt, J. L.; Wing, C. G.; Yoshida, M.; Yacamán, M. *Langmuir* **2004**, *20*, 11778. (b) Liu, L.; Zheng, H.-Z.; Zhang, Z.-J.; Huang, Y.-M.; Chen, S.-M.; Hu, Y.-F. *Spectrochim. Acta, Part A* **2008**, *69*, 701.
(11) Shang, L.; Wang, Y.; Jiang, J.; Dong, S. *Langmuir* **2007**, *23*, 2714.
(12) Medintz, I. L.; Clapp, A. R.; Mattoussi, H.; Goldman, E. R.; Fisher, B.; Mauro, J. M. *Nat. Mater.* **2003**, *2*, 630.
(13) Forster, T. *Discuss. Faraday Soc.* **1959**, *27*, 7.
(14) Lakowicz, J. R. *Principles of Fluorescence spectroscopy,* 2nd ed.; Kluwer Academic/Plenum Publishers: New York, 1999.
(15) Yun, C. S.; Javier, A.; Jennings, T.; Fisher, M.; Hira, S.; Peterson, S.; Hopkins, B.; Reich, N. O.; Strouse, G. F. *J. Am. Chem. Soc.* **2005**, *127*, 3115.
(16) Jennings, T. L.; Singh, M. P.; Strouse, G. F. *J. Am. Chem. Soc.* **2006**, *128*, 5462.
(17) Jennings, T. L.; Schlatterer, J. C.; Singh, M. P.; Greenbaum, N. L.; Strouse, G. F. *Nano Lett.* **2006**, *6*, 1318.
(18) Dulkeith, E.; Morteani, A. C.; Niedereichholz, T.; Khar, T. A.; Feldmann, J.; Levi, S. A.; Veggel, F. C. J. M.; Reinhoudt, D. N.; Moller, M.; Gittins, D. I. *Phys. Rev. Lett.* **2002**, *89*, 203002–203001.
(19) Sen, T.; Sadhu, S.; Patra, A. *Appl. Phys. Lett.* **2007**, *91*, 043104–043101.
(20) Sen, T.; Patra, A. *J. Phys. Chem. C* **2008**, *112*, 3216.
(21) Haldar, K. K.; Sen, T.; Patra, A. *J. Phys. Chem. C* **2008**, 11650.
(22) Darbha, G. K; Ray, A.; Ray, P. C. *ACS Nano* **2007**, *1*, 208.
(23) Ray, P. C.; Darbha, G. K.; Ray, A.; Hardy, W.; Walker, J. *Nanotechnology* **2007**, *18*, 375504–375501.
(24) Gersten, J.; Nitzan, A. *J. Chem. Phys.* **1981**, *75*, 1139.
(25) Persson, B. N.; Lang, N. D. *Phys. Rev. B* **1982**, *26*, 5409.
(26) Chance, R. R.; Prock, A.; Silbey, R. *Adv. Chem. Phys.* **1978**, *37*, 1.
(27) Bhowmick, S.; Saini, S.; Shenoy, V. B.; Bagchi, B. *J. Chem. Phys.* **2006**, *125*, 181102–181101.
(28) Meziani, M. J.; Pathak, P.; Harruff, B. A.; Hurezeanu, R.; Sun, Y. P. *Direct Langmuir* **2005**, *21*, 2008.
(29) Bi, S.; Ding, L.; Tian, Y.; Song, D.; Zhou, X.; Liu, X.; Zhang, H. *J. Mol. Struct.* **2004**, *703*, 37.
(30) Sahu, K.; Mondal, S. K.; Ghosh, S.; Roy, D.; Bhattacharyya, K. *J. Chem. Phys.* **2006**, *124*, 124909–124901.
(31) Tian, J.; Liu, J.; Zhang, J.; Hu, Z.; Chen, X. *Chem. Pharm. Bull.* **2003**, *51*, 579.
(32) Malicka, J.; Gryczynski, I.; Kusba, J.; Shen, Y.; Lakowicz, J. R. *Biochem. Biophys. Res. Commun.* **2002**, *294*, 886.
(33) Huang, X.; Li, L.; Qian, H.; Dong, C.; Ren, J. A. *Angew. Chem. Int. Ed.* **2006**, *45*, 5140.
(34) Bohme, U.; Scheler, U. *Chem. Phys. Lett.* **2007**, *435*, 342.

JP806866R